JOURNAL OF MATERIALS SCIENCE 24 (1989) 4509–4515

Compression fracture of organic fibre reinforced plastics

S. L. BAZHENOV, V. V. KOZEY, A. A. BERLIN
Institute of Chemical Physics, Academy of Science of the USSR, Kosygin Str. 4, 117 977 Moscow, USSR

To measure the fibre strength σ_f a new method was used and the value $\sigma_f = 450 \pm 70$ MPa was obtained. The compression strength dependence of unidirectional organic fibre reinforced plastics on the fibre volume fraction may be described by the well known mixture law. The compression strength of polyparaphenilenterephtalamid and polyparaamidobenzimidazol fibres practically coincide in spite of differences in chemical structures, tensile strengths and Young moduli. Epoxy matrix constrains the plastic fibre yield in composite and the fibre yield limit in composite is greater than the isolated fibre strength. The higher the matrix content the greater the effect. The fracture process begins with the appearance of a net of fine shear microlines, only after that do shear macrolines (so-called kinks) appear. At elevated temperatures the formation of yield macrolines is also observed but the fibre bend in the lines is symmetrical due to the symmetrical mode of fibre stability loss. The strength of organic fibre reinforced plastics is insensitive to the stress concentration effect and to the test method due to the plasticity of the composite.

1. Introduction

An important shortcoming of organic fibre reinforced plastics (OFRP) is low compression strength (5 to 7 times lower than the tensile one). Low compression strength of OFRP restricts their use in constructions which bear not only compressive but also bend load (the bend strength of OFRP is limited by its compression strength).

Compression strength of unidirectional OFRP is not higher than 260 to 310 MPa. Whether the composite strength could be increased above that value or not depends on the real value of fibre strength. In some reports the aramid fibre strength is estimated as 700 to 900 MPa [1–3] and in others as 400 to 450 MPa [4, 5]. If the effective fibre strength is equal to 400 MPa the prognosis of significant increase of OFRP compression strength would be pessimistic. One aim of this paper is to investigate the opportunity of OFRP compression strength increase and the other is the investigation of the composite fracture process.

2. Materials and experimental details

For reinforcement aramid polyparaamidobenzimidazol (PABI) and polyparaphenilenterephtalamid (PPT) fibres were used [6, 7]. Epoxy EDT-10 resin was used as a matrix. The resin was hardened at 160° C for 4 h. The samples tested were: (a) cylindrical rods 9 mm in diameter and (b) rods with rectangular cross-section (3 mm × 10 mm). The ratio of the samples diameter (thickness) to their work part length was 2.5.

Cylindrical samples were fabricated from liquid matrix impregnated unidirectionally aligned threads of fibres which were pulled into a steel pipe with 9 mm inner diameter. The excess of liquid matrix flowed out of the pipe when the fibres were pulled into it and the fibre volume fraction of composite was defined by the fibre cross-section in the prepreg. Variation of the fibre cross-section in the prepreg changed the composite fibre volume fraction. The fibre cross-section in prepreg is equal to the single fibre thread cross-section multiplied by the number of threads in the prepreg. The composite fibre content was varied from 20 to 70 vol %. The composite porosity was constant and equal to 1 to 2 vol % in the whole range of fibre volume fractions investigated.

Rectangular cross-section specimens were obtained by winding a matrix impregnated fibre thread on to a rectangular-shaped mandrel. The fibre content was varied by changing the external pressure on the fibres on the mandrel. This method does not allow the fibre content to be altered as much as the previous one without an increase in porosity at low fibre fractions.

The composite mechanical properties were measured using an Instron 1169 test machine at an upper claw velocity of 0.1 mm min^{-1}.

3. Results

3.1. OFRP mechanical properties

The dependence of composite stress on its strain is shown in Fig.1. The strain was measured by tensometer which was glued to the cylindrical work part. The stress–strain curves are typical for a plastic material. Each curve may be divided into three parts. The first part is elastic, the second plastic, stress being constant and equal to composite yield limit, and in the third part the stress diminishes. We should note the decrease of yield elongation ε_y with the increase of fibre volume fraction V_f (Fig. 1). The V_f increase also leads to a shortening of the yield segment BC in Fig. 1.

The OFRP Young modulus E_c is proportional to

0022–2461/89 $03.00 + .12 © *1989 Chapman and Hall Ltd.*

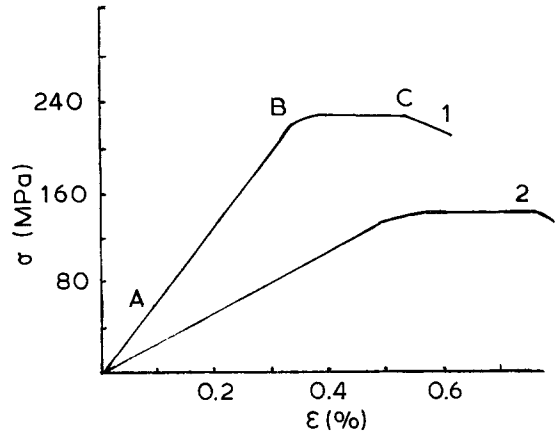

Figure 1 Stress σ versus strain ε. Fibre volume fraction 50% (1) and 30% (2),

fibre content V_f (Fig. 2)

$$E_c = V_f E_f \quad (1)$$

where E_f is the fibre Young modulus.

Extrapolation of curve 1 in Fig. 2 to $V_f = 100\%$ gives $E_f = 115$ GPa, a value which practically coincides with the fibre tension Young modulus. Thus we conclude that fibre tension and compressive moduli coincide.

OFRP compressive strength is plotted against V_f in Fig 3. An increase of V_f up to 70% leads to a linear growth of strength which may be described by the mixture law [8]

$$\sigma_c = V_f \sigma_f + V_m \sigma_m \quad (2)$$

where σ_c, σ_f and σ_m are the strengths of the composite, fibre and matrix, respectively; V_m is the matrix volume fraction.

Extrapolation of σ_c (Fig. 3) to $V_f = 0\%$ and $V_f = 100\%$ gives $\sigma_m = 85 \pm 10$ MPa and $\sigma_f = 400 \pm 40$ MPa.

It is worth noting that the compressive strengths of plastics reinforced with PPT and PABI fibres practically coincide in spite of different chemical structures and different fibre tensile strengths. We must also point out the independence of the OPRP strength on the test method (Fig. 3). For comparison the strength of glass fibre reinforced plastic (GFRP) cylindrical samples is 3 to 4 times higher than the strength of GFRP rectangular cross-section samples [9].

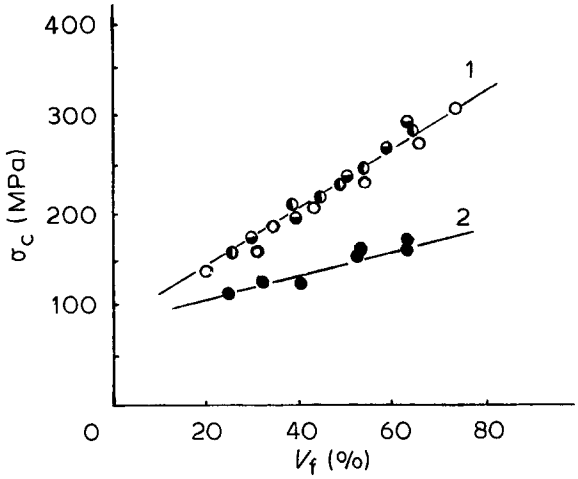

Figure 3 Organic fibre (1) and copper wire (2) reinforced plastics compression strength σ_c plotted against reinforcement content V_f. (○- PPT fibres, cylindrical samples; ◐-PABI fibres, cylindrical samples; ◒-PABI fibres, rectangular cross-section samples.)

In addition to OFRP, Fig. 3 shows the strength of a composite reinforced with plastic copper wire plotted against V_f. Extrapolation of curve 2 to $V_f = 100\%$ gives $\sigma_f = 210 \pm 30$ MPa for copper. The yield stress of copper wire can be determined independently since the yield stress of a metal at compression is equal to its tensile yield limit. The wire tensile yield stress at an elongation of 0.3 to 3% is equal to 190 to 220 MPa, a value which corresponds with σ_f obtained from Fig. 3. The supposition that aramid fibre strength is equal to 400 MPa is confirmed by analogy between OFRP and copper wire reinforced plastics fracture mechanisms. In both cases the composite strength is limited by reinforcement load capacity and in both cases the composites fracture mode is plastic with the appearance of shear yield lines.

Fig. 4 shows the elongation ε_y at which yielding begins (point B on Fig. 1) plotted against fibre content V_f. An increase of V_f leads to a significant ε_y decrease. Due to almost elastic OFRP deformation up to the beginning of its yield we can conclude that fibre yield stress in the composite is not constant and it diminishes with the growth of fibre content.

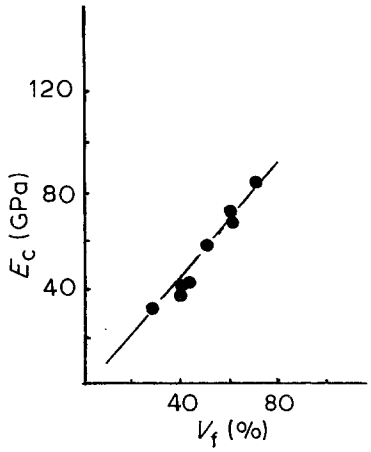

Figure 2 OFRP Young modulus E_c plotted against fibre volume fraction V_f.

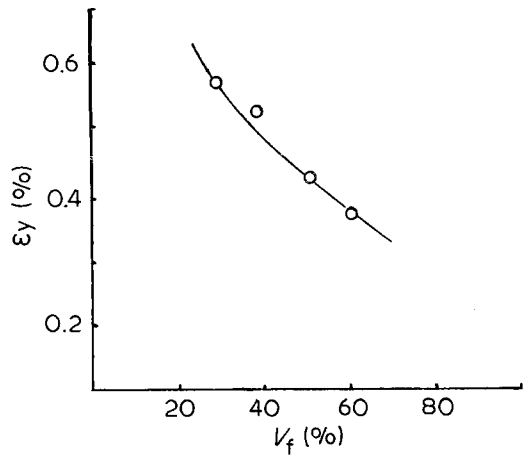

Figure 4 OFRP yield elongation ε_y plotted against fibre volume fraction V_f.

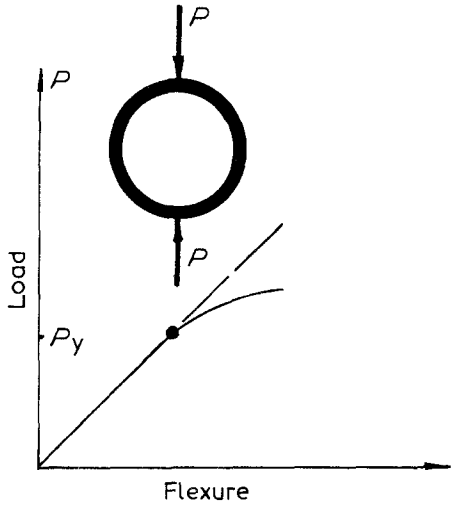

Figure 5 Compressive load P plotted against ring flexure.

3.2. Organic fibre compressive strength

Direct determination of aramid fibre compressive strength is not possible due to its small diameter, and thus different indirect methods are used. As we have noted above the values of fibre compressive strength obtained by different methods are not in agreement.

To measure the fibre strength we used a new method. For OFRP ring self-reinforced samples which consist almost of the fibres (V_f = 100%) [10] were used. Due to insufficiently high shear strength of the material which contains exactly 100% of fibres we used a composite with 95% of fibres and only 5% of the epoxy EDT-10 matrix. The matrix content in the composite is so low that it may be neglected and the material may be considered an organic "macrofibre". A measurement of the material yield stress allows the fibre strength to be determined.

Rings were compressed by two point forces (Fig. 5). When the forces are not too high a ring is elastic but at some point on Fig. 5 the dependence of force on elongation becomes non-linear. At the same moment the appearance of the first yield lines (Fig. 6a) which reveal the start of plastic deformation is observed on the ring compressed surface. A composite yield stress σ_c and its Young modulus E_c may be calculated from [11]

$$\sigma_c = 0.09\, P_y D\, h/J \quad (3)$$

$$E_c = \frac{P_y D^2}{8\, J}\,\frac{1}{5.56\lambda} \quad (4)$$

where $J = b\,h^3/12$; P_y is the load at which the yielding begins; D, b and h are the average ring diameter, its width and thickness, respectively, and $\lambda = W/D$, and W is the ring flexure.

On the basis of Equation 3 the yield limit of OFRP which contains 65% of fibres is evaluated as 290 ± 20 MPa. This value is in accordance with the composite strength at uniform compression (Fig. 3). For the composite with V_f = 95%, σ_c = 450 ± 70 MPa and E_c = 110 ± 10 GPa. The value of E_c obtained is in accordance with the aramid PABI fibres Young modulus. Thus we can conclude that the fibre yield strength is approximately 450 MPa. This estimation is in agreement with the fibre strength evaluated on the basis of the mixture law. Consequently the OFRP compressive strength is described by the mixture law and the fibre strength is equal to 400 to 450 MPa.

3.3. Fracture mechanism

The observation of the OFRP fracture process in optical and scanning electron microscope (SEM) revealed three stages.

The first stage may also be observed after flexure or uniform compression (Figs. 6a, b, and c). Fracture begins with the appearance of a net of shear microlines. The microlines are of different lengths but the shortest ones are 10 to 20 μm and their width is less than 1 μm (Fig. 6c). The microlines are associated with the plastic yielding of single or several adjacent fibres. They appear on the non-linear part of the stress-strain curve before the stress maximum at an angle of 45° ± 30′ to the load axis. The angle is the same in plastics containing 40 to 70 and 95% of fibres. Thus we may conclude that the fracture process begins from the local plastic yield of aramid fibres. It is interesting to note that at uniaxial compression in cylindrical samples shear microlines appear not uniformly over the sample but mainly in regions in which later shear macrolines ("kinks") will be formed (Fig. 6d).

The second stage is associated with the formation of one or more kinks near the stress maximum point. The width of kinks is never less than 40 to 60 μm. Their initial width is fixed but the angle θ between their plane and the load axis varies from 45° to 55°. The plastic deformation at that stage of the process is associated with the increase of the number of parallel kinks . The non-parallel kinks which intersect at some small angle were also observed.

The third stage is associated with the thickening of some kink which is accompanied by a wrinkling of fibres and microcracking of material in the kink. Just at that stage of fracture the stress on the σ–ε curve diminishes. Intersection of the adjoint kinks at an angle 70 to 90° leads to the appearance of cracks parallel to the fibre direction.

3.4. Fracture at elevated temperature

The OFRP compressive strength is plotted against temperature in Fig. 7. Abrupt strength reduction is observed near the glass transition temperature T_g (Fig. 8). It is interesting to note that if at room temperatures temperature growth leads to some strength decrease but above 110° C the strength hardly diminishes at all.

Analogously to temperature growth the reduction of deformation speed also leads to some strength decrease (Fig. 9).

We should note that near the matrix T_g the fracture mode changes, together with the change of an angle θ between the load axis and yield macrolines (Fig. 10). At elevated temperatures the yield lines are also observed but the angle θ in that case is close to 90° (Fig. 6f). At room temperatures fibre bend in the shear kink is antisymmetrical (Fig. 6e) but above T_g the fibre bend in it is symmetrical (Fig. 6f). This observation leads to the conclusion that the fracture mode changes from the exhaust of fibre load capacity at room temperatures to loss of fibre stability above T_g due to

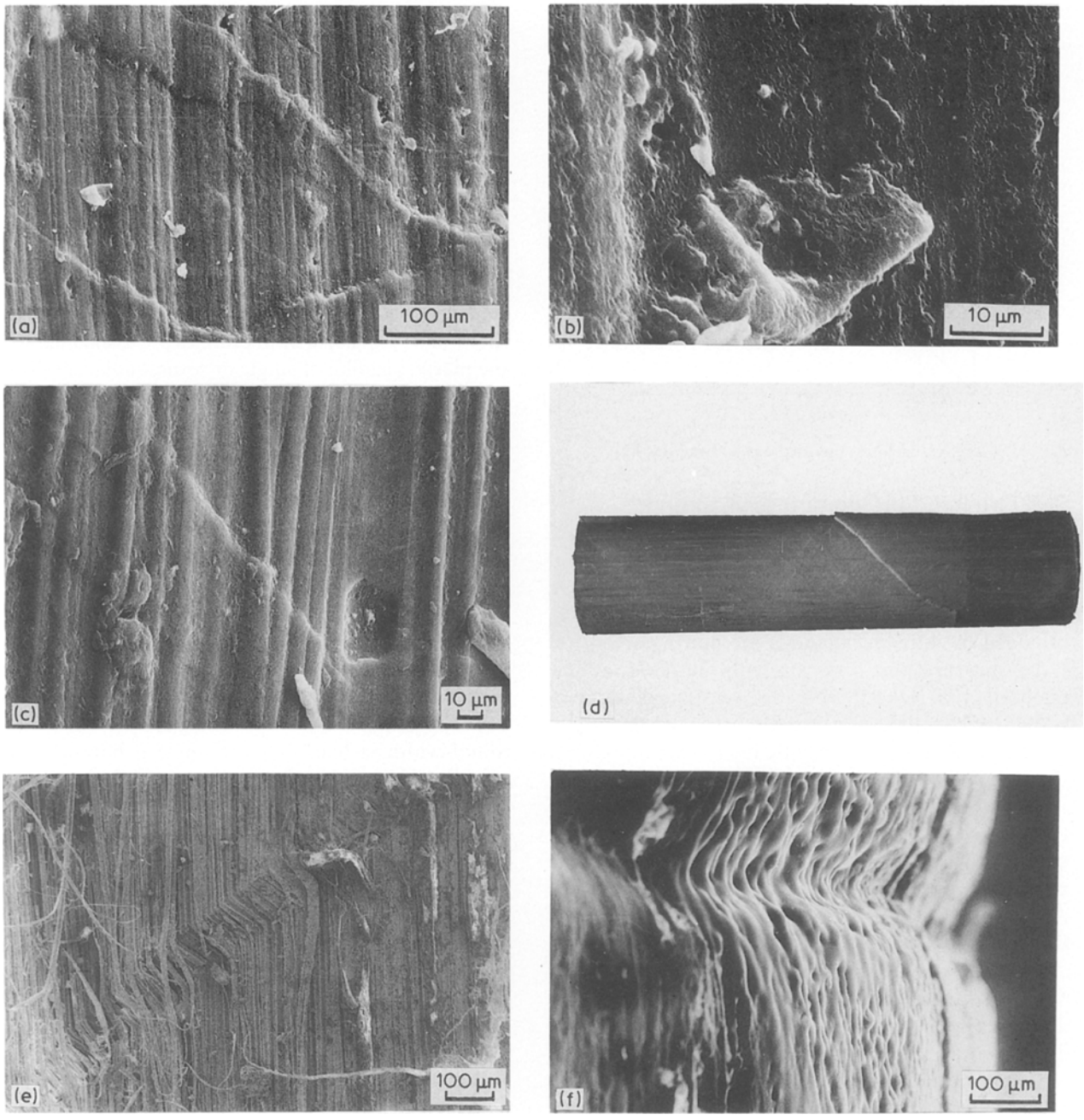

Figure 6 Yield lines in PABI fibres reinforced plastics. (a), (b) bending, $V_f = 95\%$. (c) bending, $V_f = 60\%$. (d) compression, cylindrical sample, $V_f = 60\%$. (e) kink. (f) compression at temperature 120° C, $V_f = 60\%$.

dramatically reduced matrix stiffness. The kink above matrix T_g is the wave of fibre stability loss and it may be named as "symmetrical kink".

3.5. Stress concentration influence

An investigation of stress concentrator influence on the strength of OFRP was performed on rectangular cross-section ($3 \times 10\,mm^2$) samples. Stress concentrators were circular holes and obtuse cracks. The angle in the tip of the crack was 20° to 30° (Fig. 11). If the angle of crack was lower during loading the crack shores meet and the cut part of the sample was loaded. The strength of the composite was calculated on the uncut cross-section of the samples. A plot of composite strength against crack length and hole diameter are given in Figs 12 and 13. The OFRP strength is absolutely insensitive to stress concentrator influence due to its plasticity.

4. Analysis and discussion

4.1. Mixture law and energy considerations

We must note that the mixture law describes the strength dependence not only of OFRP but also of the composite steel wire–polyester resin [12]. However, the reasons for the validity of Equation 2 in both cases are essentially different. Metal wire reinforced plastic is elastic only if the strain is less than yield strain of the wire [12]. Yielding leads to composite strengthening due to a gradually loaded matrix up to matrix yield elongation (3 to 5%). OFRP deformation has essentially different features and deformation strengthening is not observed in that composite. During loading the elastic stress is

$$\sigma = (E_f V_f + \sigma_m V_m/\varepsilon_m)\,\varepsilon \qquad (5)$$

where ε_m and V_m are matrix yield strain and its volume fraction and ε is the strain.

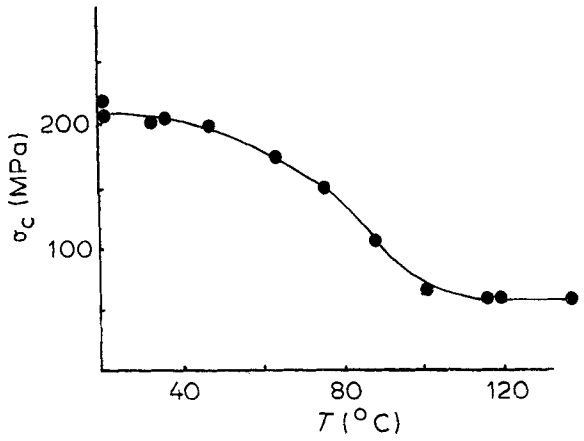

Figure 7 Compression strength σ_c plotted against temperature T. $V_f = 50\%$.

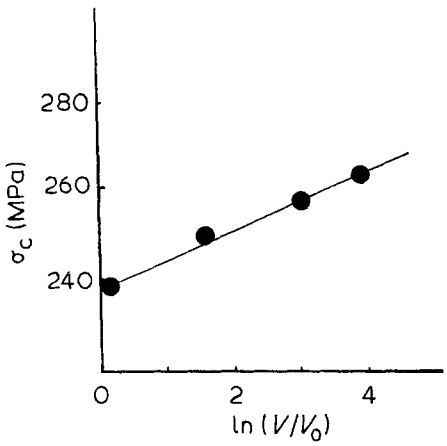

Figure 9 OFRP compression strength σ_c plotted against load velocity V.

It is essential that up to the start of the fibre yield the stress in matrix is much less in comparison with its yield limit (strength σ_m). The contradiction between mixture law and Equation 5 becomes evident if we calculate the composite stress at fibre yield elongation ε_f

$$\sigma = \sigma_f V_f + \sigma_m V_m \varepsilon_f / \varepsilon_m \quad (6)$$

where ε_m is the matrix yield strain.

For aramid fibres and epoxy matrix $\varepsilon_f = 0.3\%$, $\varepsilon_m = 4\%$ and $\varepsilon_f/\varepsilon_m \simeq 0.1$. Consequently σ in Equation 6 may be written as

$$\sigma \simeq \sigma_f V_f \quad (7)$$

Let us consider the stable yield process of the composite on segment BC in Fig. 1. If the joint yielding of fibres and matrix is taken into account the external force work must be equal to the plastic deformation work of the fibres and the matrix

$$\tau_c \, dx = V_f \tau_f \, dx + V_m \tau_m \, dx = (V_f \tau_f + V_m \tau_m) \, dx \quad (8)$$

where dx is an increment of plastic deformation; τ_c, τ_f and τ_m are the composite, fibre and matrix yield stresses, respectively.

4.2. Fibre yield limit in composite

On the basis of Equation 8 we can conclude that the composite strength σ_c which is equal to its yield stress τ_c should be calculated from the mixture law. On the other hand Equation 7 is in contradiction with energy considerations and we can suppose that composite yield deformation does not coincide with fibre yield deformation ε_f. This supposition is confirmed by direct experiments (Fig. 4). It is essential that at the start of composite yield the aramid fibre stress is higher than the yield limit of isolated fibres. This effect can be explained by the constraint influence of the matrix. The analogous effect was observed in plastic metal–metal composites at tension [13]. After the start of the matrix yield it of course, loses constraint ability.

To calculate the stress in fibres just before the start of composite yield Equations 2 and 5 were used from which we obtain

$$\sigma^f = E_f \frac{V_f \sigma_f + V_m \sigma_m}{V_f E_f + V_m E_m} \simeq \sigma_f + \sigma_m V_m / V_f \quad (9)$$

Where $\sigma_m V_m / V_f$ is the fraction of fibre strength in composite which is due to the matrix constraint effect. If V_m is low $\sigma^f = \sigma_f$ and fibre strength in composite is equal to strength of isolated fibre. On the other hand if $V_m \gg V_f$ the strength increase effect cannot be neglected. This is the reason why measuring fibre strength by means of bending an elastic beam with a

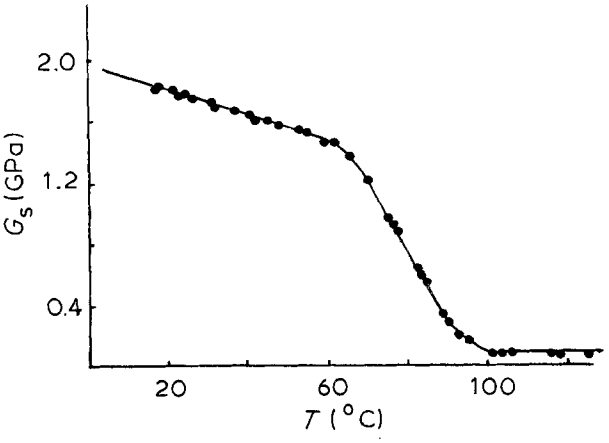

Figure 8 OFRP modulus of elasticity at torsion G_s plotted against temperature T.

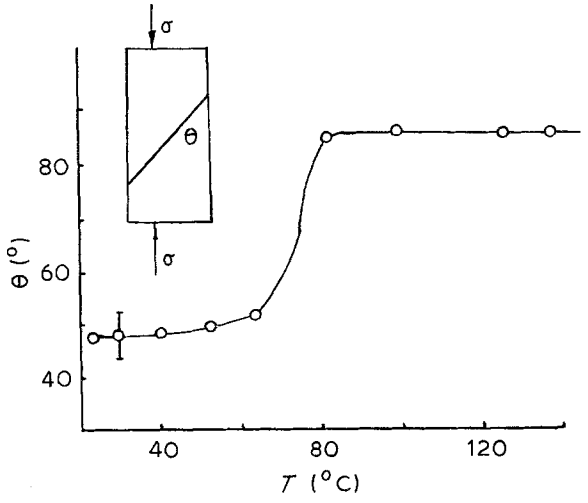

Figure 10 Angle between yield line and load axis θ plotted against temperature T.

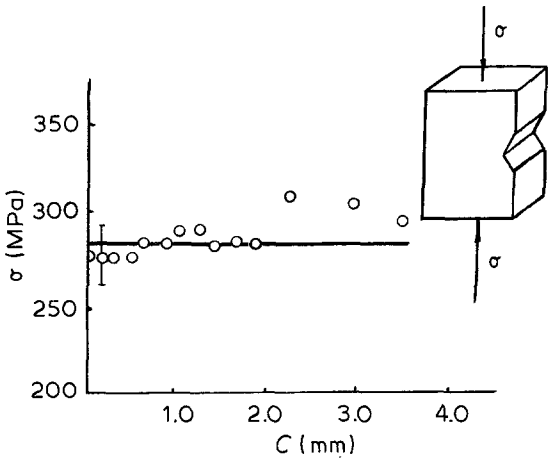

Figure 11 Compression strength σ plotted against crack length C.

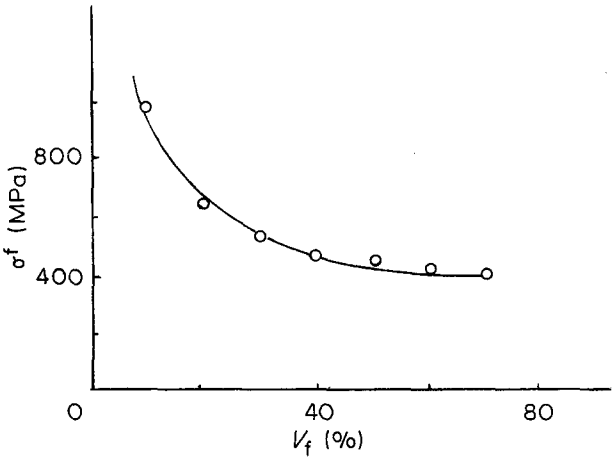

Figure 13 Yield stress of PABI fibres in composite σ^f plotted against fibre volume fraction V_f.

fibre glued to it [3] leads to significant overestimation of σ_f (700 MPa). The fibre yield stress in OFRP plotted against fibre volume fraction V_f is shown in Fig. 1.

If the first yield lines appear at stress σ_f in one or several adjacent fibres they have to go through the matrix also. In spite of very low average composite strain (0.3%) the local matrix shear deformation in yield lines is high enough and matrix shear stresses in yield lines are equal to its yield limit. For this reason yield lines growth stops unless the stress is described by mixture law.

We must note that first yield lines in aramid fibres appear at relatively low stresses. However, the fibre yield in that case is not uniform (Fig. 6d). SEM investigation of aramid fibres revealed intensive fibre yielding only in the kink regions. Far from the kinks the yield lines were not observed at all. In spite of the appearance of first yield lines at relatively low stresses the fibre yielding in that case is not general due to the matrix constraint effect. This fact confirms the conclusion about growth of fibre yield stress in composites.

4.3. OFRP strength prognosis

The value of aramid fibre strength 400 to 450 MPa obtained does not allow hope for the significant increase of the OFRP compressive strength in the near future as the load capacity of the fibres considered is already completely realized in the composite. Some strength increase can be obtained by using strong polymer matrix but the effect in that case cannot be more than 10 to 20%.

The only way to increase the OFRP strength is to enhance the fibre compressive strength. However, it looks doubtful due to the insensitivity of the fibre strength to the variation of chemical structure of the fibres. The examples are PPT and PABI fibres which are considered in the present paper and polybenzothiazole fibres [14].

The low compressive strength is the shortcoming not only of the organic fibres but also of PAN-based carbon fibres. If the latest technological successes of carbon fibres the main result of which was a significant increase of fibre tensile strength were followed by essential growth of compressive strength the analogue successes in chemistry of aramid fibres were not followed by any growth of compressive strength at all. It is possible to suppose that in the near future the OFRP compressive strength will hardly increase.

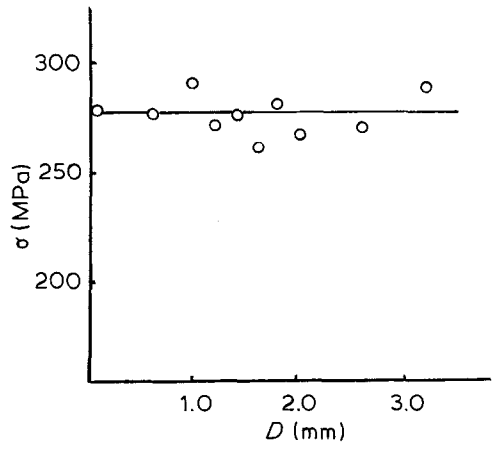

Figure 12 Compression strength σ plotted against cylindrical hole diameter D.

4.4. Fracture mechanism

The investigation of the OFRP fracture process has shown three different modes of plastic deformation. The first is the appearance of shear lines which are typical for plastic polymers and the second is the kink formation typical for composites only. Kinks appear near the maximum stress point and their broadening leads to the composite load capacity loss. The third mode of yield is associated with fibre stability loss at elevated temperatures when the yield lines are oriented almost perpendicularly to the fibre axis. In this case the lines are the waves of fibre stability loss and the fibre bend in the yield lines is symmetrical.

The typical angle between load axis and the kink plane is 48° to 52° but the kinks appearing at the angle of 45° were also observed. The following explanation of the angle θ instability cause may be valid. Apparently some kinks are formated from the long enough shear lines and the angle θ in this case is exactly 45°, but in other cases a kink may arise from not very long shear lines and the penetration of kink through the sample may be defined by some stress concentration in

the kink tip. In that case the maximum shear stress does not necessarily coincide with the 45° direction.

5. Conclusions

The conclusions are as follows.

1. The dependence of OFRP compressive strength plotted against fibre volume fraction is described by the mixture law.

2. Aramid fibre compressive strength is equal to 400 to 450 MPa.

3. The strengths of PABI and PPT fibres coincide.

4. Epoxy matrix constrains the yield line formation in the fibres. Due to this effect the fibre yield stress in composites is greater than the isolated fibre strength. The higher the matrix content the higher is the constraint effect.

5. At elevated temperatures the fracture mode changes from exhaust of fibre bearing capacity to the fibre stability loss.

6. There are three different modes of plastic deformation: (a) shear on fine yield lines; (b) shear on antisymmetrical kinks; (c) yield on symmetrical kinks at elevated temperatures.

7. Due to OFRP plasticity its strength is insensitive to the stress concentrator effect and to the test method.

References

1. J. H. GREENWOOD and P. G. ROSE, *J. Mater. Sci.* **9** (1974) 1804.
2. A. A. ASLANIAN, S. L. BAZHENOV, A. J. GORENBERG, A. M. KUPERMAN, A. A. BERLIN and E. S. ZELENSKIJ, *Dokl. Akad. Nauk SSSR* **291** (1986) 1113 (in Russian).
3. J. DETERESA, S. R. ALLEN, R. J. FARRIS and R. S. PORTER, *J. Mater. Sci.* **19** (1984) 57.
4. V. V. KOZIJ, S. L. BAZHENOV, A. M. KUPERMAN, A. A. BERLIN and E. S. ZELENSKIJ, *Dokl. Akad. Nauk SSSR* **298** (1988) 62 (in Russian).
5. S. R. ALLEN, *J. Mater. Sci.* **22** (1987) 853.
6. G. I. KUDRIAVTSEV, A. V. TOKAREV, L. V. AVRAROVA, V. A. KONSTANTINOV, *Him. Volokna* **N.6** (1974) 70 (in Russian).
7. G.A.BUDNITSKIJ, *ibid.* **N.2** (1977) 11 (in Russian).
8. C. C. CHAMIS, in "Fracture and Fatigue" (Academic Press, New York, 1974) p. 106.
9. A. M KUPERMAN, S. L. BAZHENOV, A. A. ASLANIAN, A. A. BERLIN and E. S. ZELENSKIJ, *Dokl. Akad. Nauk* **298** (1988) 1424.
10. E. F. KHARCHENKO, S. L. BAZHENOV, V. D. PROTASOV and A. A. BERLIN, *Mechanica Kompozitnih Mater.* **N.2** (1987) 345 (in Russian).
11. A. A. NIKISHIN and A. L. RABINOVICH, in "Teoretichna i pri-lozhna Mekhanika Vol. 1 (BAN, Sofia, 1971) p. 113 (in Bulgarian).
12. E. M. DE FERRAN and B. HARRIS, *J. Compos. Mater.* **4** (1970) 62.
13. S. T. MILEIKO, *J. Mater. Sci.* **4** (1969) 974.
14. R. J. DIEFENDORF, in "Carbon Fibres and Their Composites" (Springer, Berlin, 1985) p. 46.

Received 15 June
and accepted 7 December 1988